

# BUNCH COMPRESSOR FOR HIGH-CURRENT SINGLE BUNCH ELECTRON LINEAR ACCELERATOR

Seishi TAKEDA, Toshihiko HORI, Kunihiro TSUMORI, Tamotsu YAMAMOTO,  
Tokuo KIMURA, Tomikazu SAWAI, Juzo OHKUMA, Setsuo TAKAMUKU,  
Toichi OKADA, Koichiro HAYASHI and Masaharu KAWANISHI

Radiation Laboratory  
The Institute of Scientific and Industrial Research  
Osaka University, Ibaraki, Osaka 567, JAPAN

## Abstract

A bunch compressor with four dipole magnet has been installed and tested on the ISIR-Osaka single bunch electron linear accelerator. The single bunch with a full length of 40 ps is compressed into 12 ps, whereas the bunch length of 16 ps in FWHM is compressed into 9.5 ps. The maximum compression rate is estimated to be about 30 % for the single bunch with the charge of 10-40 nC.

## Introduction

The performance of a linear collider is strictly limited by the deleterious effects of the longitudinal and the transverse wake fields generated by high-current bunches in the linear accelerators.<sup>1-2</sup> The longitudinal wake fields affect the energy spread of the bunch, whereas the transverse wake fields increase the beam emittance. These two wake fields depend on the longitudinal charge distribution of the bunch and the amplitude of the wake fields increases with the bunch intensity. For high-current bunches, longer bunch lengths result in less energy spread than short bunch lengths, since the longitudinal wake potential decreases with increasing bunch lengths. On the other hand, shorter bunch lengths are preferable to reduce emittance growth due to the transverse wake fields. If the charge distribution of the single bunch can be controlled, the optimum balance of two deleterious effects both by the longitudinal and the transverse wake components will be obtained.

The energy spectrum of the single bunch accelerated in the linear accelerator is determined by both the accelerating field and the longitudinal wake potential. The minimum energy spread is obtained, when a single bunch is accelerated ahead of the rf crest.<sup>3-6</sup> The energy of the head of the bunch is lower than the average energy, while the tail of the bunch is accelerated at higher energy.

A bunch compressor consisting of four dipole magnets is designed to produce an achromatic bump in the beam trajectory. Figure 1 shows a principle of the bunch compressor. The low energy electrons take a longer path through the bunch compressor than the high energy electrons. After passing through the bunch compressor, distance between the high energy electrons and the low energy electrons will be shortened, and then the bunch length will be compressed. The bunch length of the high-current single bunch will be reduced by a bunch compressor.

## High-Current Single Bunch Electron Linear Accelerator

The ISIR-Osaka Single Bunch Electron Linear Accelerator<sup>7</sup> produces a high-current single bunch by means of the subharmonic prebuncher (SHPB) system. The linear accelerator consists of a 120 keV electron gun, three SHPBs, a prebuncher, a buncher, a 3 m long accelerating waveguide, a bunch chopper, a bunch compressor and a transport system. The accelerating waveguide is driven by a 20 MW L-band klystron, and both the buncher and the prebuncher are driven by a 5 MW L-band klystron.

The single bunch of 16 - 20 ps bunch length and up to 67 nC in bunch charge, with the energy spread of 0.7 - 2.5 % over the range of 24 - 34 MeV, and the repetition rate from a single shot to 720 pps can be accelerated. The normal operating energy and the energy spread depend on the single bunch charge, since the energy spread is determined by both the accelerating field and the longitudinal wake potential. The single bunch of 67 nC, 16-20 ps with a long tail, 24-28 MeV, 2.5 % energy spread is obtained. However, the single bunch of 25-45 nC in charge are used for the experiments in routine work, since the minimum energy spread of 0.7 % is obtained at 33 nC. The beam emittance of  $\pi$  mm-mR is observed for the single bunch of 10 nC, 16 ps, 24-34 MeV, 1 % in energy spread.

## Subharmonic Prebuncher System

As shown in fig. 2, the system consists of a 12th SHPB followed by a 180 cm drift tube, a 12th SHPB followed by a 120 cm drift tube and a 6th SHPB with a 80 cm drift tube. These three SHPBs are coaxial single-gap cavities, with 3.4 cm gap at one end of the inner conductor. The frequencies, number and locations of SHPBs, and the optimum values of voltages and RF phases in the cavity gaps have been chosen by the results of the computer simulation. A one-dimensional disk model has been used to calculate the longitudinal space-charge debunching forces present in a high-current beam inside a cylindrical conducting tube.

The loaded figure of merit  $Q$  is estimated to be 4,400 for the 12th SHPB cavities and 1,970 for the 6th SHPB cavity. The inner conductors of the cavities are made of copper solid tubes and the outer conductors are made of copper cylinder clad by a SUS tube. The conducting drift tubes of smaller diameter are required

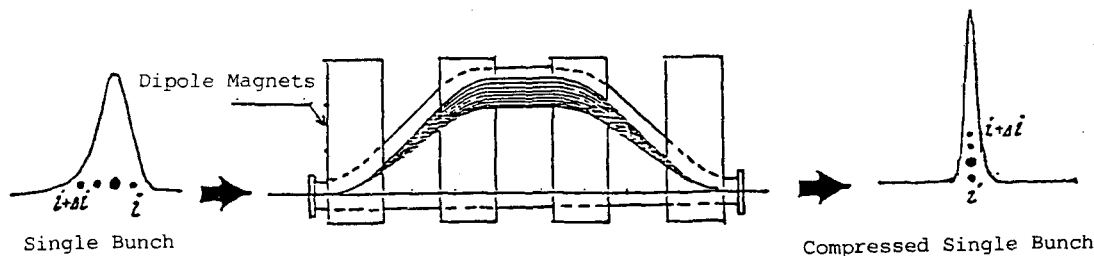


Fig.1 The principle of the bunch compressor.

to reduce the forces due to space-charge debunching whereas the larger diameter is preferable for the effective vacuum pumping. The inner diameter of the conducting tube is 5 cm. The conductance and the inductance for the image charge flow induced by the high-current beam should be reduced since the wake fields give rise to produce unstable beam. The drift tubes between SHPBs are made of copper clad by SUS tube and the vacuum stations are connected with the drift tubes through the conducting copper slits.

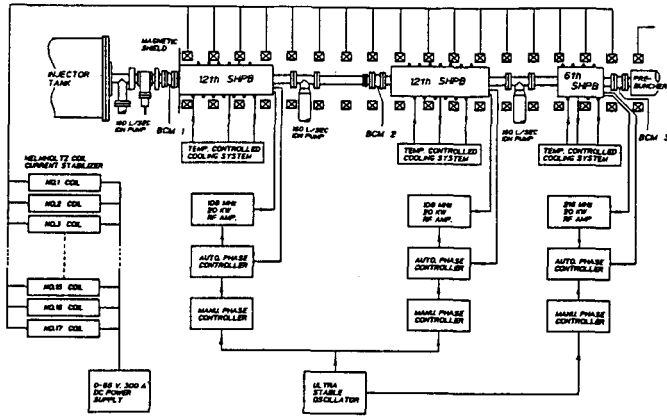


Fig.2 The subharmonic prebuncher system.

These three SHPBs are independently connected with the rf amplifiers which generate the rf up to 20 kW in a pulse of 20 sec. Each amplifier is excited by a master oscillator that produces rf signals at 108.4 MHz and 216.8 MHz. The rf phases and the rf powers can be independently controlled by the manual operation at console desk in order to obtain optimum subharmonic bunching. The stabilities of the intensity and the energy spectrum are obtained by minimize the drift of the rf phases between cavity gaps. The automatic phase controllers are installed in the amplifiers in order to lock the rf phases at the cavity gaps.

The subharmonic prebunchers and the drift tubes are confined by the Helmholtz coils, which are independently connected with the power supplies. The axial magnetic fields are tapered from 150 Gauss at the entrance to 540 Gauss at the output in order to keep the beam at Brillouin flow condition as the charge density increases due to subharmonic bunching. The electron gun is placed in a magnetic shield, while the field strength is about 60 % of the Brillouin flow condition. The beam from the gun is focused by two magnetic lenses in order to control both the radius and the convergence of the beam at the entrance to the magnetic confined region.

The electron beam up to 30 A in a pulse of 4.5 ns is generated from the thermionic electron gun. The beam is partially bunched by two 12th SHPBs and then the beam is bunched by the 6th SHPB into the acceptance angle (0.5 ns) of the prebuncher. It is equivalent that the pulse beam up to 300 A in a pulse of 0.5 ns from the gun is injected into the prebuncher. The final bunching before injection into the 3 m long accelerating waveguide is performed with a traveling wave buncher.

#### Bunch Chopper

A bunch chopper driven by the 24th subharmonic frequencies (54 MHz) is installed at the down stream of the accelerating waveguide. One of the multi-bunches up to 11 bunches is selected at the beam window or at the energy analyser in order to investigate the effects of the wake fields between multi-bunches.

#### Wake field Induced by High-Current Single Bunch

If a single bunch passes through an accelerating structure of linear accelerators, the wake field is generated as the result of interacting with the cavity. The wake fields generated by an electron in the single bunch give rise to the forces on the successive electrons in the single bunch. The wake potential  $W(t)$  over all length in the linear accelerator is defined as the potential experienced by a test electron following a distance,  $ct$  behind the head of the bunch.

For a low-current single bunch, the longitudinal wake potential is lower than the accelerating voltage in the linear accelerator. The energy spread is determined both by the bunch length and the rf phase where the bunch is accelerated. For a high-current single bunch, the longitudinal wake potential increases by the collective effect. The total energy gain of an electron at time  $t$ , can be determined by adding the longitudinal wake potential to the external accelerating voltage,

$$E(t) = E_0 \cos(\omega t - \theta) + W(t),$$

where  $\theta$  is the phase-angle between the single bunch and the accelerating voltage. With increase of bunch charge, the wake potential  $W(t)$  increases from the small fraction of the accelerating voltage to the value which is large enough to distort the net accelerating voltage.

The shape of the bunch accelerated by the linear accelerators is not a Gaussian-like shape but a gamma function-like shape with a bunch tail, which is expressed as the following function;

$$I(t) = k(t-t_v)^A \text{Exp}[-(t-t_v)/B],$$

where  $I(t)$  is the current waveform of the bunch,  $k$ ,  $A$  and  $B$  are constants to determine the bunch shape, and  $t_v$  is the appearance time of the bunch head. The expression of the gamma function is linearized by logarithmic transformation and then the function is fitted to the observed bunch shape using a weighted least squares method.

The longitudinal wake potential of the single bunch passed through a 3 m long accelerating waveguide is calculated by time domain analysis using vector potential.<sup>8-9</sup> The typical longitudinal wake potential for the single bunch of 16 nC ( $1 \times 10^{11} e^-$ ) is shown in fig.3. The minimum energy spread can be obtained, when the single bunch is accelerated at the positive phase-angle where the negative going slope of the accelerating voltage waveform is made to cancel with

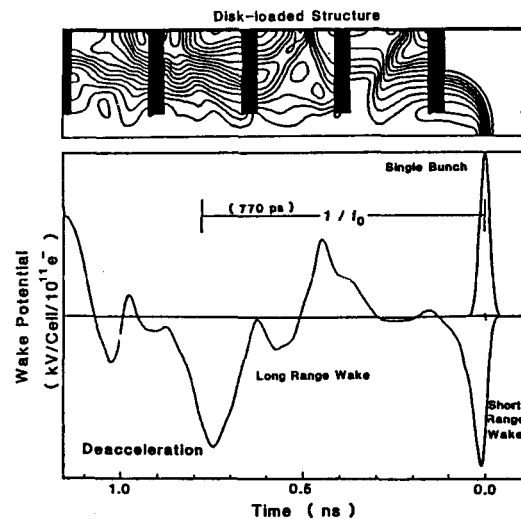


Fig.3 The longitudinal wake potential of the single bunch in the L-band linear accelerator.

the positive going slope of the wake potential. The optimum phase angle ahead of the crest which minimizes the energy spread increases with the single bunch charge and the average energy of the bunch also decreases.

#### Bunch Length Measurements System

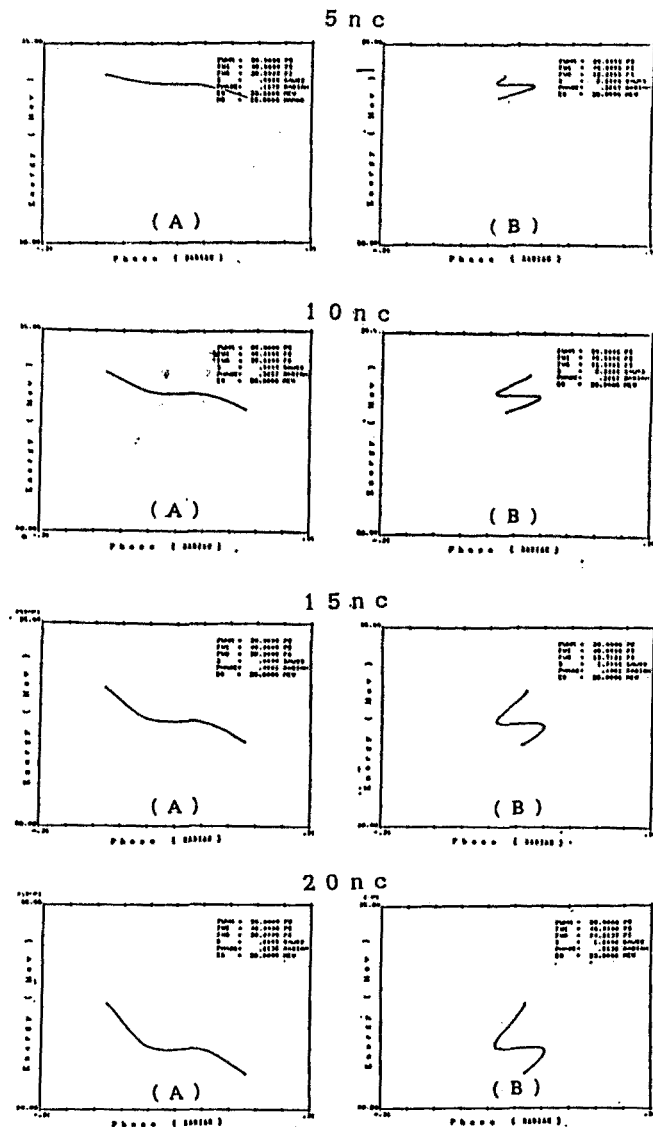
In order to measure the bunch length, the bunch waveform should be detected with the time resolution of the order of ps. In such a short time scale, the optical detection system is more effective than the electric detection system.<sup>10</sup> As the index of the air is 1.00027311 at 1 atm and 20 °C, the electrons with the energy higher than 21.36 MeV radiate the Cerenkov in the air. The Cerenkov angle is estimated to be 0.69°, 0.93° and 1.05° at 25 MeV, 30 MeV and 35 MeV respectively. The Cerenkov light at the beam window is guided to a observation room with plane mirrors and a lense made of VUV grade fused quartz (Suprasil) lense. Finally, the Cerenkov light-beam is focused by a Suprasil lense into the slit of a streak camera (Hamamatsu Photonix, C1370-01) which has a time resolution of 2 ps.

The C1370-01 streak camera consists of VUV lenses and P11 photocathode, and then the sensitivity region in wavelength is 185 - 850 nm. As the optical index of refraction  $n$  in the fused quartz depends on the wavelength, the light of continuous wavelength such as the Cerenkov light gives rise to the transit time spread. The transit time spread between 185 nm and 850 nm wavelength is estimated to be 1.8 ps/cm in the VUV (Suprasil) lenses installed between the beam window and the streak camera. In order to avoid the transit time spread, an interference filter which transfers 38 % of photons in the wavelength between 425-435 nm is installed in front of the slit. The slit width of the streak camera is adjusted to be 4-5  $\mu\text{m}$  so as to obtain the time resolution of 2 ps.

The streak image on the fluorescent screen of the streak camera is transferred to a data processing system (Hamamatsu Photonix, C1098) by a SIT camera. The streak camera is triggered by a signal obtained from a beam current monitor at the exit of the accelerator. The jitter of the streak image is observed to be about 10 ps, which is determined by an internal jitter of the streak camera. As the decay of the SIT camera is about 0.6 s, the streak image of oneshot without jitter can be obtained at the repetition rate lower than 1.5 pps. The rf power is supplied to the linear accelerator with the repetition rate of 10 pps, while the beam injection from the gun is operated at 1.1 pps so as to obtain the oneshot streak image.

#### Bunch Compressor

The bunch compressor consists of four dipole magnets which produces an achromatic bump in the bunch trajectory such as an energy compressor system (ECS). By placing the single bunch at the optimum phase-angle where the energy spectrum is minimized, the tail of the bunch will be higher in energy than the average energy, while the head of the bunch will be lower than the average energy. The higher energy electrons take a shorter path through the compressor than the average energy electrons. On the other hand, the lower energy electrons take a longer path through the compressor than the average energy electrons. As the result, the tail of the bunch will catch up the head of the bunch, and the head of the bunch will fall behind the bunch. The bunch length will be shortened with increasing magnetic field strength of the bunch compressor. For the higher field strength of the magnet, the bunch tail will pass bunch head, and the bunch head will fall behind the bunch tail. As the result, the bunch length increases.



(without bunch compressor) (with bunch compressor)

Fig.4 The single bunch expressed in the energy-phase space with/without the bunch compressor.

The effect of the bunch compressor for the single bunch both with the bunch width of 16 ps in FWHM and with the full width of 40 ps full width is calculated for various single bunch charge. The longitudinal wake potential is calculated for the single bunch passing through a 3 m long L-band linear accelerator with the time domain analysis. In order to minimize the energy spectrum, the single bunch should be accelerated at the positive phase-angle where the negative going slope of the accelerating voltage waveform is made to cancel with the positive slope of the longitudinal wake potential. Figure 4 shows the single bunch with the minimum energy spread expressed in the energy-phase space. The energy of the bunch tail is higher than the average energy while the energy of the bunch head is lower than the average energy. The optimum phase angle ahead of the crest which minimizes the energy spectrum increases with the single bunch charge from 5 nC to 20 nC. With increasing the single bunch charge, the average energy decreases and the energy difference between the bunch head and the bunch tail increases. Figure 5 shows the compressed bunch length in full width for the magnetic strength of the bunch compressor. The magnetic

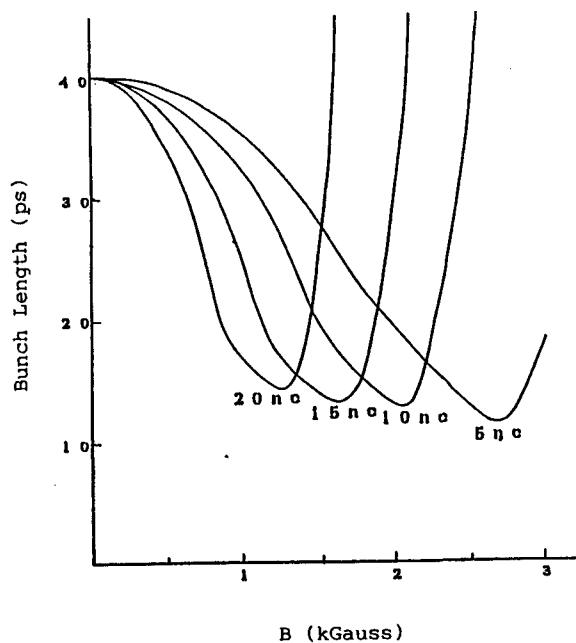


Fig.5 The compressed bunch length in full width for magnetic strength of the bunch compressor.

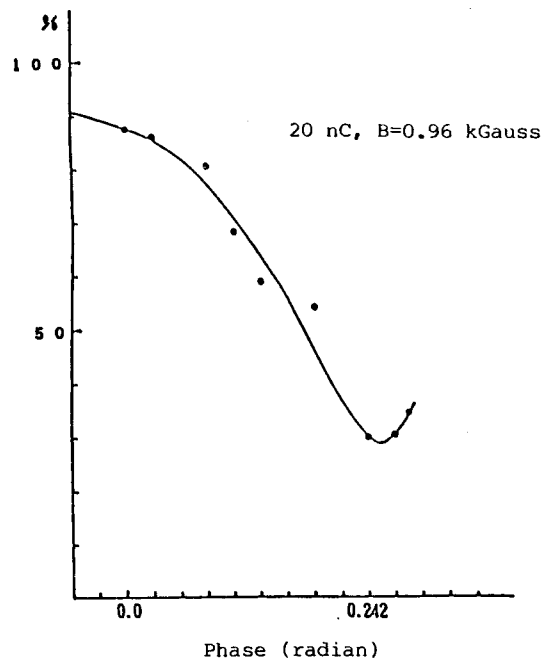


Fig.7 The compression rate and the phase where the single bunch is accelerated.

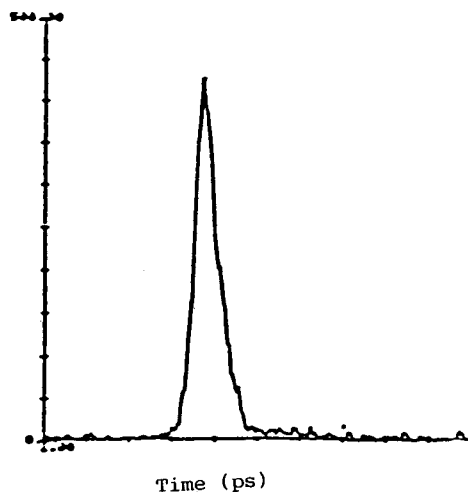
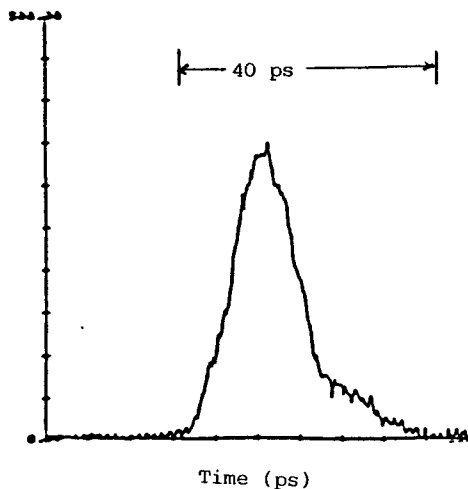


Fig.6 The shape of the single bunch with/without the bunch compressor.  $B=0.96$  kGauss, Phase=0.242 radian.

strength at the minimum bunch length decreases with increasing charge, since the difference of the energy between the bunch tail and the bunch head increases with charge.

Figure 6 shows the typical bunch waveforms with/without the bunch compressor. The single bunch charge of 20 nC is accelerated at the phase-angle of 0.242 radian from the crest. The single bunch with a full length of 40 ps is compressed into 12 ps, whereas the bunch length of 16 ps in FWHM is compressed into 9.5 ps. The maximum compression rate of the single bunch is about 30 % for the single bunch with the charge of 10-40 nC.

#### References

1. G.A.Loew, SLAC-PUB-3892 (1986).
2. P.B.Wilson, SLAC-PUB-3674 (1985).
3. S.Takeda, N.Kimura, K.Tsumori and M.Kawanishi, Proc. 4th Symp.on Accel.Sci.and Tech. (IPCR, 1982) 79.
4. S.Takeda, KEK Report 84-16 (Nov. 1984) 77.
5. G.A.Loew and J.Wang, SLAC/AP-25 (1984).
6. J.E.Clendenin, S.D.Ecklund, M.B.James, R.H.Miller, J.C.Sheppard, J.Sodja and J.B.Truher, SLAC-PUB-3285 (1984).
7. S.Takeda, K.Tsumori, N.Kimura, T.Yamamoto, T.Hori, T.Sawai, J.Ohkuma, S.Takamuku, T.Okada, K.Hayashi and M.Kawanishi, IEEE Trans. Nucl. Sci. NS-32, No.5, (1985) 3219.
8. T.Shintake, KEK-Report 84-15 (1984).
9. S.Takeda, N.Kimura, K.Tsumori, M.Kawanishi and T.Shintake, Proc. 5th Symp. on Accel. Sci. and Tech. (KEK, 1984) 80.
10. S.Takeda, KEK Report 81-16 (1982) 18.